

Experimental Characterization of Carbon Nanotube Field Emission Cathode Lifetime

Logan T. Williams¹ and Mitchell L. R. Walker²

High-Power Electric Propulsion Laboratory, Georgia Institute of Technology, Atlanta, Georgia, 30332

Victor S. Kumsomboone³ and W. Jud Ready⁴

Georgia Tech Research Institute, Atlanta, Georgia, 30332

There is interest in the use of carbon nanotubes (CNTs) to create a field emission cathode for small satellite applications and the neutralization of exhaust plumes of low-power electric propulsion devices since field emission cathodes do not require a gas flow to operate. As a part of the cathode's development, the current emission output over the lifetime of the cathode must be determined. The Georgia Tech Research Institute and the Georgia Tech High-Power Electric Propulsion Laboratory have fabricated multiple field emission cathodes that consist of multi-walled CNT arrays. Seven cathodes are characterized at pressures below 10^{-5} Torr at constant voltage between the CNTs and the gate until failure occurs. The maximum current density observed is 9.08 mA/cm^2 , the maximum power density is 9.08 W/cm^2 , and the maximum life-span is 368 hours. The behavior of the cathode current emission consists of oscillations and sudden shifts thought to be caused by CNT interactions. Resistive heating is thought to be the primary cause for failure.

I. Introduction

THE use of carbon nanotubes (CNTs) for field emission (FE) cathodes holds great potential as a general electron emitter, especially in the area of electric propulsion (EP). There is a need for an efficient electron source to neutralize the exhaust plume of low-power EP devices ($< 500 \text{ W}$).¹ Most thrusters operate in conjunction with thermionic hollow cathodes, which require a gas flow in order to emit electrons. For a hollow cathode in use with a 200-W Hall effect thruster, which requires 0.8 A of cathode current, the propellant flow rate through the cathode is typically 10% of the flow through the thruster itself.² In addition, hollow cathodes require heating as well as a biased keeper to ignite and initially sustain the cathode until the cathode is hot enough to self heat. A FE cathode only requires an electric field for extraction of electrons. Since most spacecraft that use low-power EP systems have limited power capacity and spacecraft mass allotment, this makes the simpler setup of the FE cathode a more attractive alternative. Beyond the advantages from a systems design standpoint, FE cathodes can be very durable, as CNTs are both chemically and mechanically robust.³ Recent work demonstrates the potential of FE cathodes not only in the areas of low power EP, but also in the areas of propellant-less propulsion such as space tethers, and spacecraft charge control.^{1,4}

Field emission is the extraction of electrons from a conductive material through quantum tunneling. The application of an external electric field lowers the potential barrier to the point that the transmission probability of an electron becomes non-negligible. Field emission devices share the common feature that the emission sites are small points which focus the electric field lines and increase the local electric field strength. This focusing effect allows for low macroscopic electric field strengths ($\sim 1 \text{ V}/\mu\text{m}$) to enable electron emission. This focusing effect is termed the field amplification factor. Past designs of FE cathodes consist of a base material, generally a doped n-type semiconductor, with a layer of emitter of material on top. A conductive screen, termed the gate, placed above the emitter is the extraction electrode. The electric field is applied between the emitter material and the gate. Spindt developed the first FE cathodes in the late 1960's which used metal cones as the emitter material. Subsequent FE cathode designs use different emitter materials, including films made from diamond and CNTs.^{3,5-9} Past work by

¹ Graduate Research Assistant, Aerospace Engineering, lwilliams@gatech.edu, AIAA Member.

² Assistant Professor, Aerospace Engineering, mitchell.walker@ae.gatech.edu, Senior AIAA Member.

³ Research Assistant, Georgia Tech Research Institute, victor.kumsomboone@gtri.gatech.edu.

⁴ Senior Research Engineer, Georgia Tech Research Institute, jud.ready@gtri.gatech.edu.

Williams *et al* studied the performance of vertically aligned CNT array FE cathodes.¹⁰ This current work studies the current emission of seven CNT cathodes at constant voltage between the CNTs and the gate over time until emission ceases.

II. Experimental Design

The CNT cathode follows the Spindt design pattern where the cathode consists of a base, an insulator layer, and a gate layer. Multi-walled CNT arrays are grown on the base to serve as emitters. An electric field is generated between the nanotubes and the gate to extract the electrons from the CNT tips. The insulator electrically isolates the base from the gate. Figure 1 shows a cut-away representation of the cathode design.

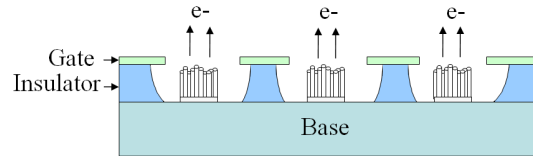


Figure 1. Design configuration for CNCC.

The cathode fabrication process consists of successive layer deposition. The base is a wafer of n-type silicon selected for electron donation. The insulator layer is made of silica (SiO_2) and is thermally grown 10 microns thick atop the silicon. The gate layer is formed by the deposition of a 200 nm thick layer of chromium with electron beam evaporation. Silica and chromium are used as they do not inhibit CNT nucleation or growth.¹¹ The chromium surface is then covered with photoresist. A pattern of a repeated shape is made in the photoresist by photolithography, which defines the shape of the nanotube arrays. The array patterns are defined by shape size (such as length or diameter as appropriate) and pitch (the separation distance between the centers of adjacent arrays). After the pattern is developed, the chromium gate is etched away via a standard chromium etch process. The SiO_2 insulator is etched via reactive ion etching. Since the etch rate differs between the two materials, more of the silica is removed than the chromium. Thus, the gate layer extends over the recesses of the insulator. The etched Cr and SiO_2 allow a line-of-sight path for the deposition of an iron catalyst layer directly on the silicon. The photoresist and excess iron are removed via a stand liftoff process using sonication in acetone. The CNTs are grown with chemical vapor deposition (CVD) in a quartz furnace with methane, acetylene, and hydrogen.¹²

Figure 2a shows images of circular CNT arrays from one of the samples tested. Figure 2b shows a closer view of the nanotube morphology obtained with a scanning electron microscope (SEM). The arrays demonstrate a degree of overall uniformity in shape, although there is a slight variation between some arrays. Fringe nanotubes exist at the edges of the arrays that are not vertically aligned with the array. The individual nanotubes that make up the arrays have an outer diameter of about 20 nm. The density of the nanotubes within each array is about 10% by area, which means that each nanotube is about 70 nm apart. Despite the overall structure of the CNT arrays, the individual nanotubes display a kinked vine-like morphology and have a degree of anisotropy.¹² A summary of the geometry of the samples tested is outlined in Table 1.

The process used in this work created nanotubes that extend beyond the gate, seen in Figure 2(a). The resultant arrays have a height of about 50 microns, rather than the expected 5-10 microns. Thus the resultant CNT samples did not exactly match the original design. The design illustrated in Figure 1 is an example of an intrinsic cathode,

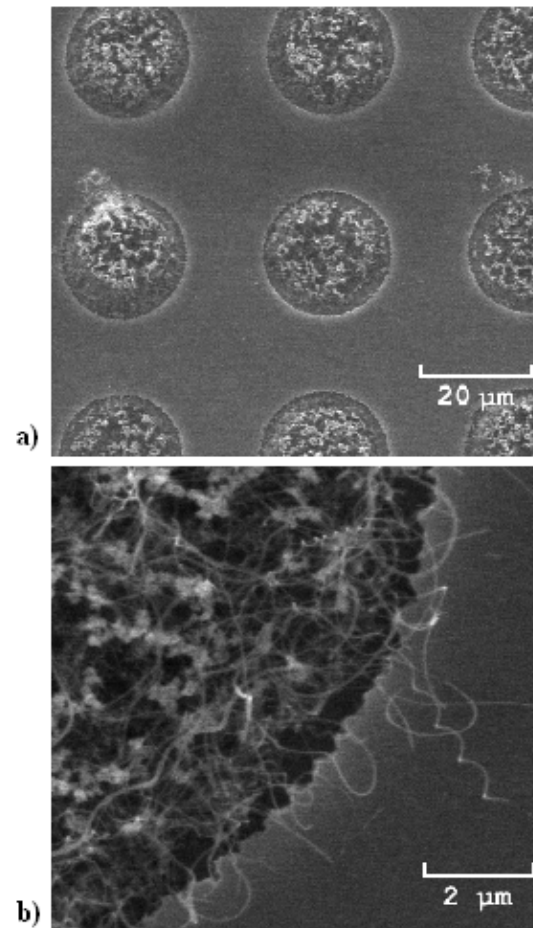


Figure 2. Micrographs of CNT arrays (a) Non-uniformity of arrays, (b) fringe CNTs near the edge of an individual array.

where the nanotube arrays are entirely recessed within the insulator. In order to generate an electric field that emits electrons downstream of the cathode, an external gate is suspended above the surface of the wafer. The electric field is created between the external gate and the CNT arrays rather than the chromium gate as outlined earlier. This setup is referred to as the extrinsic configuration.

The wafer that contains the CNT arrays is mounted on an aluminum body with Pelco colloidal silver liquid. The gate is a 0.035 mm thick molybdenum grid with 0.14 mm hexagonal holes with a 0.025 mm edge-to-edge separation. The gate is mounted 1.3 mm above the surface of the wafer. The cathode is then mounted in the vacuum chamber.

III. Experimental Apparatus

A. Vacuum Facilities

All experiments are conducted in a 0.5 m diameter by 0.7 m tall stainless-steel bell jar vacuum system. Figure 3 shows a diagram of the bell jar vacuum system. The bell jar is evacuated with a Varian VHS-6 diffusion pump which is mechanically backed by an Alcatel 2033 SD rotary vane pump. An uncooled optical baffle prevents oil from back-streaming into the bell jar. The diffusion and backing pumps have pumping speeds (for air) of 2400 l/s and 8.33 l/s, respectively. Pressure in the bell jar is measured by a Bayard Alpert 571 ion gauge in connection with a SenTorr ion gauge controller with an overall error of 20%,¹³ as well as two Varian 531 thermocouple pressure transducers connected to Varian Model 801 thermocouple gauge controllers.

B. Experimental Apparatus

The 1 cm by 1 cm silicon wafer which contains the CNTs fits into a stainless steel mount which is mounted on an aluminum bracket with four 2-56 size nylon machine screws to maintain electrical isolation. Another aluminum bracket is placed 2.5 cm opposite from the face of the cathode body as an anode. Figure 4 shows the triode configuration used to connect the cathode, gate, and anode. The anode bias voltage, V_a , is supplied by a Xantrex XPD 60-9 power supply. The cathode bias voltage, V_c , is supplied by a Kepco BHK 2000-0.1MG power supply. Both the anode and cathode power supplies share the same ground. The currents to the gate, anode, and cathode are measured across three 1-k Ω current shunts with a combination of a Fluke multi-meter and an Agilent 34970A data acquisition unit (DAQ). The resistance value has a tolerance of $\pm 5\%$, the multi-meter has an uncertainty of 0.1%, and the DAQ has an uncertainty of 0.004% for an overall uncertainty in the current density measurement of 5%.

D. Procedure

In order to study current emission, each sample is individually tested in the bell jar vacuum system. The chamber is evacuated to a pressure below 1×10^{-5} Torr. The anode is biased to 50 V, and the cathode voltage is progressively increased in 50 V steps at 5 minute intervals to at least 1000 V. The current is measured every five

Table 1. Cathode CNT array patterns.

Sample	Pattern Shape	Pattern Size (μm)	Pitch (μm)	CNT Area (cm^2)
1	Triangle	4	16	0.0091
2	Diamond	8	64	0.0056
3	Diamond	2	8	0.0181
4	Star	8	32	0.0070
5	Star	50	150	0.0200
6	Diamond	1	8	0.0056
7	Square	4	16	0.0181

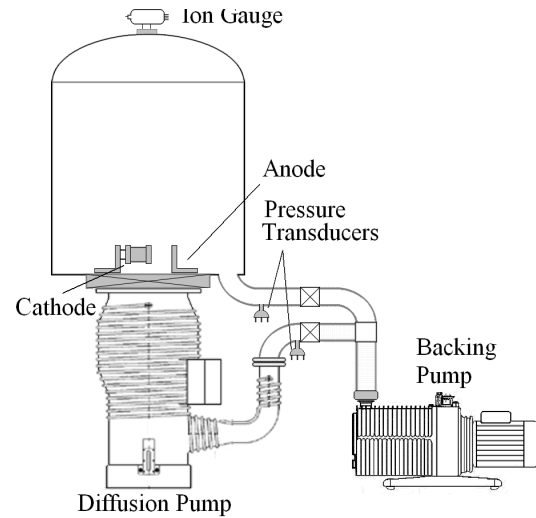


Figure 3. Diagram of the bell jar vacuum system.

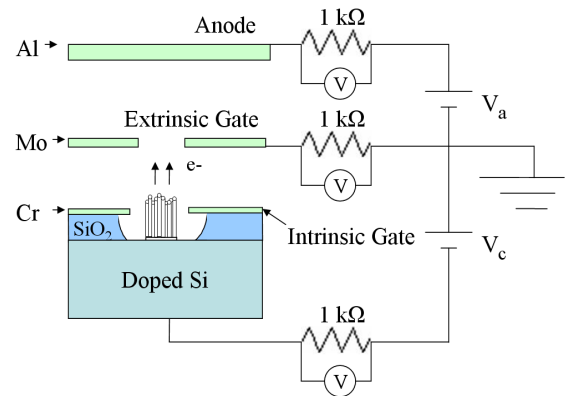


Figure 4. Cathode electrical schematic.

minutes until the cathode ceases to emit. The average current density is calculated as the current output divided by the area of the CNT arrays.

IV. Experimental Results

Figure 5 shows the current density emitted by each cathode sample over time. One common characteristic between all of the current emission of the samples over time is the existence of discontinuous jumps in the current emission, particularly just before the sample fails. Some samples demonstrated multiple shifts in current emission, such as samples 2, 3, 4, and 7. Table 2 shows a summary of the performance of the samples in terms of the cathode lifetime, the maximum current density emitted, and the maximum power density of the emitter.

Another major characteristic of the measured current densities is that many has an oscillatory nature. Samples 1 and 6 both have a single dominant oscillation combined with a slowly changing DC component, while samples 2 and 4 have a sum of several oscillations at different frequencies combined with a DC component.

Figure 6 shows the current emission of each cathode normalized by the maximum recorded value and plotted against normalized time. This was done to demonstrate the similarities between samples and to better see the shape of trends in the emission current. Between samples 2, 4, and 5 each cathode experienced a sudden drop in current emission at about 85% of the total lifetime.

All the cathodes demonstrate similar behavior of the ratio of the anode current to the total current emitted from the CNTs, called the transmission ratio. The higher the transmission ratio, the greater the percentage of the electrons emitted are available for an application. In each case, the plots of current versus time for both the anode and the gate currents have the same shape. If the current collected by the anode drops, the current collected at the gate experiences a similar drop. The offset between the two, related to the transmission ratio, is not constant

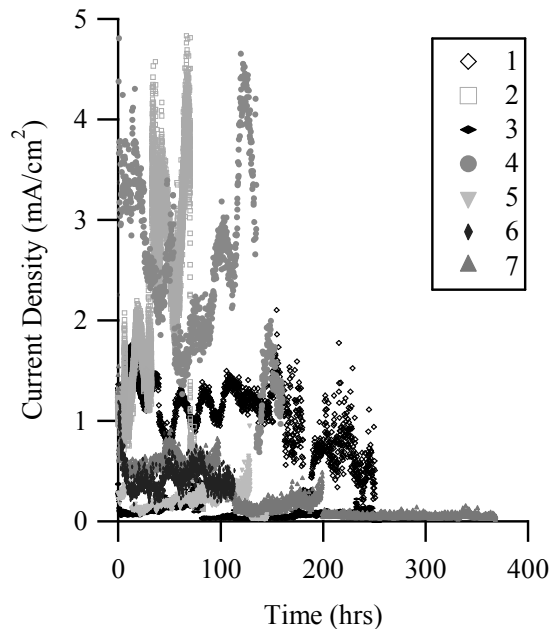


Figure 5. Summary of CNT cathode emission.

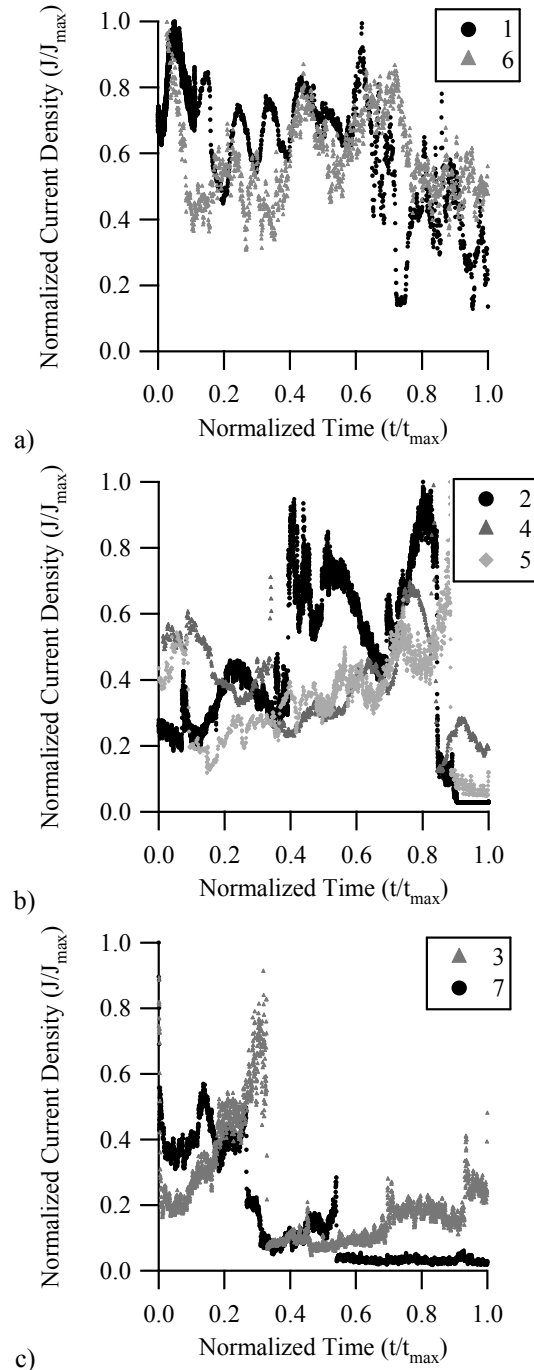


Figure 6. Normalized current as a function of normalized time density at constant voltage.

however. A common feature in the samples is that the transmission ratio is initially around 50%, and then decreases in an exponential fashion. Whenever the current emission undergoes a shift, the transmission ratio likewise shifts. Generally after each such shift the variance of the transmission ratio increases. Figure 7 shows a plot that illustrates both common features.

V. Discussion

There are two features of cathode operation over the lifetime that are learned from the data: the failure mechanism and the steady state behavior of the cathode. The failure mechanism is most likely resistive heating. There is ample evidence of thermal damage, and cathode lifetime decreases as the cathode power density increases. The behavior of the current emission over time is not a function of the initial geometry of the CNT arrays. With the composition of the CNTs being consistent, it is thought that current switching caused by interactions between nanotubes are the cause for the varying behavior between samples.

A. Failure Mechanism

The first piece of evidence about the failure mechanism is that many of the samples underwent shifts in current emission at the same normalized time. While the current density shifts did not always occur at the same relative time, the fact that shifts overlapped the majority of the time suggests that the phenomenon is rate dependent, rather than a function of absolute time. This means that nanotube failure is a result of some physical process within the nanotubes. The data also shows that this process is related to the power density applied through the emitter, since cathode lifetime decreases as average power density increases. This suggests resistive heating, which is the process where Ohmic heating from the current passing through the nanotubes heat the tubes and enhance oxidative ablation, or outright vaporize the outer wall.¹⁴ A higher power density causes a higher current flowing through a given number of nanotubes. Since individual nanotubes have the same diameter, neglecting the slight variations in height between nanotubes, a higher power density would result in a faster rise in temperature in the nanotubes. This in turn increases the rate of oxidative ablation and vaporization. After each test the anode contains a film of carbon, which confirms that CNT material is vaporized and ejected from the cathode during operation.

Another piece of evidence that suggests resistive heating is the presence of thermal damage on the face of the emitters. Figure 8 shows a compilation of optical microscope images of sample 4 that show regions of scorching on the right half of the wafer. Damage of this kind is present on every sample, which suggests that there are regions of high thermal deposition. This supports the idea that resistive heating is the mechanism in question. The existence of multiple scorch marks suggests that there are clusters of CNT arrays that act as primary emitters. As current is emitted, heat is transferred from the CNT arrays to the surrounding material, causing the thermal damage. The reason for multiple scorches is that as one region fails another activates, causing thermal damage in another location.

Resistive heating is not the only thermal event that occurs. One possibility is that resistive heating might lead to arcing, as the vaporization of the nanotube walls from resistive heating might create a conductive path to the gate. Figure 9 shows a region of sample 1 that has a solidified flow from melting the silicon substrate in the center of a scorch mark. The high temperature needed to melt silicon (1420 °C) suggests that arcing occurred at that point, rather than some other phenomenon. Gröning *et al* determined that arcing in a CNT film cathode could create currents as high as 8×10^5 mA/cm² in 200 ns pulses that could deposit $10^4 - 10^5$ J/cm³.¹⁵ Such an arc could cause the damage seen in Figure 9, and a 200 ns pulse would not be registered by the DAQ unit. Such arcing potentially

Table 2. Cathode Performance.

Sample	Life (hrs)	Max Current Density (mA/cm ²)	Average Power (W/cm ²)
1	250	2.10	1.45
2	83	4.83	2.73
3	249	0.50	0.10
4	117	9.08	2.52
5	145	0.95	0.27
6	113	0.44	0.53
7	368	1.54	0.21

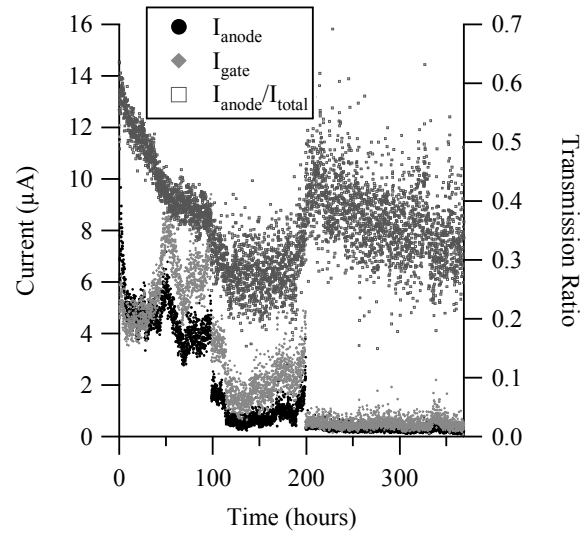


Figure 7. Transmission ratio of sample 7. Anode voltage 50 V, cathode voltage 1200 V.

occurs when vaporized CNT material creates a conductive pathway to the gate.¹⁴ Work by Sowers shows that for the case of a diamond film cathode, arcing decreased the electric field required to extract electrons, which Sowers attributed to a reshaping of the film to include more jagged points. Whether this type of structural reshaping occurs in CNT films is unknown. The shifts in current emission could also be due to arcing damaging the emission sites, which would result in the activation of other emission sites that might not have as high a local field amplification factor. Therefore an arc between the gate and the cathode could cause large changes in current emission by either altering the shape of the CNTs and increasing the field amplification factor or by changing emission sites after an arcing event. However, as there is no evidence of widespread arcing, resistive heating is thought to be the dominant mechanism for failure.

There are several alternative failure mechanisms that were considered and rejected. Work by Bonard¹⁴ suggests several different mechanisms by which CNT emitters may fail. Of the various means explored by the literature, those most applicable to the observed emission currents are wall shedding of multi-walled nanotubes (MWNT) into single-walled nanotubes (SWNT) and arcing between the nanotubes and the gate. While it is tempting to consider another of Bonard's mechanisms, failure due to mechanical stresses, it did not seem particularly feasible in this situation. Failure caused by mechanical stresses has generally been associated with CNT films, where the nanotubes are not arranged in a given orientation and are forced into a vertical position by the applied electric field. In this case, the CNTs are grown in vertical arrays. While the kinked morphology might introduce some strain as the nanotubes straighten in the electric field, the stress would be much lower than in CNT films. Additionally, the cathodes operated at electric field intensities much lower than what Bonard observed for failure ($\sim 1 \text{ V}/\mu\text{m}$ versus $3 \text{ V}/\text{nm}$ for Bonard).

Other hypothesized failure modes in the literature only explain slight variations in the current emission. Some of the basic failure modes for single-walled nanotubes, such as selective oxidation, ion bombardment, and field evaporation, might be the cause for minor fluctuations in the current emission of the cathodes.¹⁸ While no experiments have been done to tie such mechanisms to multi-walled nanotubes (MWNTs), it is a simple matter to consider their impacts on MWNTs. Should an outer wall of a MWNT be weakened by an ion impact or from oxidation, a section of the nanotube could be ejected and follow the electric field lines to the anode. The departure of a section of a MWNT would disturb the local electric field lines and thus the current emission from the nearby nanotubes. Likewise, current saturation and breakdown of the CNTs might be a factor.¹⁶ However, these mechanisms would only describe moderate fluctuations in the current emission, and would particularly not explain the large discontinuities in current emission seen in samples 2, 4, and 5 as that would imply a large number of nanotubes are shedding the outer walls at the same time. Such an occurrence, while possible, would be unlikely considering that it would require a very large number of active emission sites.

Most likely the length of the nanotubes is the ultimate cause for the failure of the cathodes. In terms of resistive heating, an increase in nanotube length increases the resistance and thus the heat generated. The increased amount of material also increases the likelihood of vaporized CNT material forming a conductive path to the gate and initiating arcing. A refinement of the fabrication process to reduce the CNT height to the designed value should greatly reduce the above processes and increase cathode life span.

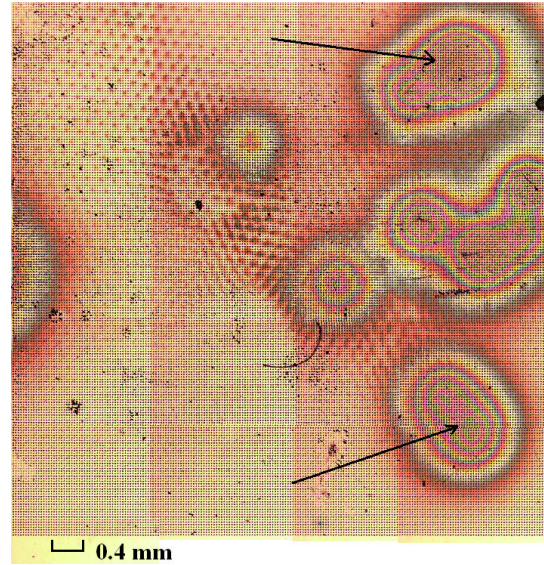


Figure 8. Thermal damage on sample 4. Arrows drawn point to the scorch marks.

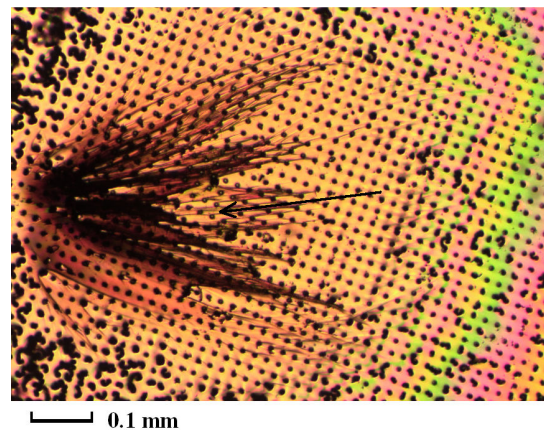


Figure 9. Melted substrate on sample 1. Arrow points to melted substrate.

B. Cathode Geometry and Current Switching

The geometric configuration of the arrays has no direct effect on the behavior of the current emission over time. Work by Suh *et al* demonstrates that CNTs are sensitive to field screening effects for nanotubes as sparse as one per $50 \mu\text{m}^2$.¹⁷ For comparison, the samples tested have a nanotube density of one per $0.001 \mu\text{m}^2$, and array densities between one per $16 \mu\text{m}^2$ and one per $5625 \mu\text{m}^2$. The expectation is that the array geometry or structure may have some impact on the current emission, as field screening effects vary with array size and pitch. However, some samples with similar behavior of the current emission have completely different geometric characteristics. As an example, sample 2 consists of arrays that individually have incomplete growth, yet shows similar behavior to sample 4, which has arrays that are overgrown. The only observable geometric correlation is that as the area occupied by the nanotubes increases, the lifetime of the cathode increases. This makes sense, as the smaller the area, the greater the power per unit area extracted from the cathode.

While the behavior of the current emission varies between cathodes, the behavior of the transmission ratio is very similar between samples. It would be expected that the transmission ratio would be constant, as the geometry of the gate does not change. However, not only is the transmission ratio not constant, it behaves the same way for each sample. The decrease in the transmission ratio might be not due to the deposition of material on the grids, which would physically decrease the amount of free space for the electrons to pass through. The same gate is used for each sample, and the transmission ratio each time would initially have a value between 0.5 and 0.6, which is higher than some of the minimum values observed. This instead suggests some mechanism involving the CNTs. Similarly, it is not understood why the transparency would change after any sudden shift in current emission. When this occurs, the transmission ratio changes from an exponential decay in time to a linear change in time, if not constant. As these traits were present in all samples, the phenomenon seems to be independent of CNT geometry.

It is possible that the varying behavior of the current emission is a result of interactions between CNTs. In addition to the fact that the geometry has no effect on the behavior of the current emission, all the samples were created using the same process, so individual CNT composition is the same. One possible explanation is that the CNTs undergo current switching. Current switching is a sudden change in current emission caused by changes in the emitting CNT tip. Current switching can be caused by motion of the nanotube, as different facets of the CNT structure have slightly different work functions. Collins and Zettl¹⁸ show that current switching caused by interactions between nanotubes could shift current emission by an order of magnitude in only a few seconds. Since small perturbations could have a large effect on current emission, it is possible that the behavior of the current emission between samples diverges as CNTs start to interact in a non-linear fashion. Such CNT interactions explain the observed oscillations as an oscillation in the tip interactions between CNTs.

VI. Conclusion

Seven CNT cathodes fabricated from vertically aligned arrays are operated at constant voltage between the gate and CNTs over time to provide current densities up to 4.24 mA/cm^2 and power densities of up to 4.24 W/cm^2 for lifetimes up to 368 hours. The current emission over time is characterized by oscillations and sudden shifts, with resistive heating as the primary cause for failure. The behavior of the cathodes over time is independent of initial CNT geometry and are thought to be determined by current switching caused by CNT interactions.

Acknowledgments

The authors of this paper would like to thank Prof. Lisa Pfefferlee of Yale University for technical assistance, the Georgia Tech Aerospace Engineering Machine Shop for fabrication and hardware support, and the graduate students of the High-Power Electric Propulsion Laboratory for additional assistance. This work is sponsored by DARPA per contract number HR0011-07-C-0056.

References

- ¹Mueller, J., Marrese, C., Wirz, R., Tajmar, M., Schein, J., Reinicke, R., Hruby, V., "JPL Micro-thrust Propulsion Activities," *Proc. NanoTech*, 2002.
- ²Hargus, W. A., and Reed, G., "The Air Force Clustered Hall Thruster Program" *Proc. 38th AIAA/ASME/SAE/ASEE Joint Propulsion Conf. and Exhibit*, 2002.
- ³Gasdaka, C. J., Falkos, P., Hruby, V., Robin, M., Demmons, N., McCormick, R., Spence, D., Young, J., "Testing of Carbon Nanotube Field Emission Cathodes," 2004.
- ⁴Gilchrist, B. E., Jensen, K. L., Gallimore, A. D., Severns, J. G., "Space Based Applications for FEA Cathodes (FEAC)," *Materials Research Society Symposium Proceedings*, Vol. 621, 2000.

- ⁵Spindt, C. A., Holland, C. E., Rosengreen, A., Brodie, I., "Field-Emitter Arrays for Vacuum Microelectronics," *IEEE Transactions on Electron Devices*, Vol. 38, No. 10, 1991, pp. 2355-2363.
- ⁶Agüero, V. M., Adamo, R. C., "Space Applications of Spindt Cathode Field," *6th Spacecraft Charging Technology Conference Proceedings*, 2000, pp. 347-352.
- ⁷de Heer, W.A., A. Chatelain, and D. Ugarte, "Carbon nanotube field-emission electron source," *Science*, Vol. 270, No. 5239, 1995, pp. 1179.
- ⁸Gamero-Castaño, M., Hruby, V., Falkos, P., Carnahan, D., Ondrusek, B., Lorents, D., "Electron Field Emission from Carbon Nanotubes, and its Relevance in Space Applications," *Proc. 36th AIAA/ASME/SAE/ASEE Joint Propulsion Conference*, 2000.
- ⁹Sowers, A. T., Ward, B. L., English, S. L., and Nemanich, R. J., "Field emission properties of nitrogen-doped diamond films," *Journal of Applied Physics*, Vol. 86, No. 7, 1999, pp. 3973-82.
- ¹⁰Williams, L., Kumsomboone, V. S., Ready, W. J., Walker, M. L. R., "Experimental Characterization of a Carbon Nanotube Field Emission Cathode", *Proc. 44th AIAA/ASME/SAE/ASEE Joint Propulsion Conference*, 2008.
- ¹¹Hofmann, S., et al., "Direct growth of aligned carbon nanotube field emitter arrays onto plastic substrates," *Applied Physics Letters*, Vol. 83, No. 22, 2003 pp. 4661-4663.
- ¹²Turano, S. P., Ready, J., "Chemical Vapor Deposition Synthesis of Self-Aligned Carbon Nanotube Arrays," *Journal of Electronic Materials*, Vol. 35, No. 2, 2006
- ¹³Varian, Vacuum Measurement, In Varian, Inc., 2003
- ¹⁴Bonard J. and Klinke C., "Degradation and failure of carbon nanotube field emitters," *Physical Review B*, Vol. 67, 2003.
- ¹⁵Gröning, O., Küttel, O. M., Schaller, I., Gröning, P., and Schlapbach, L., "Vacuum arc discharges preceding high electron field emission from carbon films," *Applied Physics Letters*, Vol. 69, No. 4, 1996, pp. 467-468.
- ¹⁶Collins P. G. *et al*, "Current saturation and electrical breakdown in multiwalled carbon nanotubes," *Physical Review Letters*, Vol. 86, No. 14, 2001, pp. 3128-3131.
- ¹⁷Suh, J. S., et al., "Study of the field-screening effect of highly ordered carbon nanotube arrays," *Applied Physics Letters*, Vol. 80, No.13, 2002, pp. 2392-2394.
- ¹⁸Collins P. G. and Zettl A., "Unique characteristics of cold cathode carbon-nanotube-matrix field emitters," *Physical Review B*, Vol. 55, No. 15, 1997, pp. 9391-9399.